High-frequency stabilization and high-order harmonic generation of an excited Morse oscillator under intense fields

T. F. Jiang
Institute of Physics and Department of Electrophysics, National Chiao Tung University, Hsinchu 30050, Taiwan, Republic of China
(Received 13 January 1993)

We study the quantum dynamics of a Morse oscillator under an intense field with three different frequencies: (1) one much higher than the dissociation energy from an excited state, (2) one resonant with the dissociation energy from an excited state, and (3) an intermediate one. The calculations were performed by using the *momentum-space* Fourier-grid Hamiltonian method. The high-frequency stabilization and harmonic-generation spectra are shown. The laser frequencies discussed are currently experimentally available.

PACS number(s): 33.80.Wz, 33.90.+h

Recent theoretical studies showed that atoms under a very strong high-frequency field will be relatively stable against ionization [1]. But the predicted frequency leading to stabilization is much higher than the ionization potential [2]. This kind of laser frequency required for stabilization for systems prepared in the atomic ground states is not available in current laser sources. Incidentally, the dissociation dynamics of a diatomic molecule under intense laser shows similar characteristics of atomic strong-field phenomena [3]. It would be interesting to study the corresponding molecular stabilization against dissociation with the currently available laser sources. The present study is oriented along this line. Another interesting phenomenon of current atomic physics study is the high-order harmonic-generation effect in strong fields [4]. There are many reports on harmonic generation for atoms, but few for molecules [5].

In a previous study of strong-field effects on a one-dimensional hydrogen atom, we explored the advantages of the momentum-space representation for treating the nonperturbative time-dependent problem [6]. We develop here the Fourier-grid Hamiltonian method [7] in momentum space (p-FGH). It preserves the excellent properties of momentum-space representation, and more importantly, the number of grid points required to reach excellent accuracy is significantly reduced. The p-FGH method associated with complex scaling and Floquet theory has been used by Yao and Chu in studying the stability of Cl^- in 193-nm intense laser fields [8]. In this study, we integrate the time-dependent Schrödinger equation for a driven Morse oscillator directly in momentum space with the Fourier grid. The system has many bound states in addition to the continuum instead of the single-bound-state system such as Cl^- [9]. Also, the pulse shape to model the experimental source is considered.

The purposes of this article are threefold: (1) First, we study the stabilization of an excited Morse oscillator. With the parameters of HF molecule and prepared in the lowest 14th vibrational state, the current ArF excimer 193-nm laser provides the ratio of photon energy to dissociation energy at 5.6. It satisfies the criterion of high-frequency stabilization and can be examined experimentally. We choose this initial state because the excitation of the HF molecule from the 14th vibrational state has been studied before [10]. (2) Second, we study the multiphoton dissociation from the same state but with 1074- and 532-nm wavelength lasers. From this study we can examine the frequency effects on stabilization. (3) Finally, we study the high-order harmonic generations in both cases.

With the current short-wavelength ir and excimer laser sources, the dipole approximation is adequate. The model Hamiltonian of a Morse oscillator with dipole moment d_1 in the electromagnetic field can be written as

$$H = \frac{p^2}{2m} + D(1 - \exp^{-\alpha(x-x_0)})^2 - \frac{d_1 A \cdot p}{m}, \tag{1}$$

where D is the dissociation energy, x_0 is the equilibrium nuclear separation, m is the reduced mass, and A is the vector potential. For HF molecular vibrational states, the physical parameters are $D = 0.225$, $x_0 = 1.7329$, $\alpha = 1.1741$, $d_1 = 0.31$, and $m = 1744.7$ (atomic units are used throughout the paper). The Morse potential supports 24 bound states.

To give a simple interpretation for the high-frequency stabilization, consider the Morse oscillator in the intense sinusoidal field $E(t) = E_m \sin(\omega t)$. It has been shown that the Schrödinger equation under the Kramers-Henneberger frame is in the following form [1,11]:

$$i(\partial/\partial t)|\psi\rangle = (p^2/2m)|\psi\rangle + V(x + \alpha(t))|\psi\rangle, \tag{2}$$

where

$$\alpha(t) = (E_m/m\omega^2)\sin(\omega t) = \alpha_0 \sin(\omega t). \tag{3}$$

So $V(x+\alpha(t))$ is periodic and can be written in Fourier series form:

$$V(x + \alpha(t)) = \sum_{n=-\infty}^{n=+\infty} V_n(\alpha_0; x) e^{-in\omega t}. \tag{4}$$

In the high-frequency regime, the $n \neq 0$ terms in Eq. (4) oscillate rapidly and can be neglected in the zeroth-order approximation. In Fig. 1 we show the field-deformed potential $V_0(\alpha_0; x)$ at a fixed intensity for both 1074-nm and 193-nm cases. The dissociation limit of the 1074-nm case decreases about 35% while the potential curve for the 193-nm case is almost unchanged. This illustrates that the high-frequency case is relatively stable compared to the low-frequency one.

We then choose a laser pulse with electric field

$$E(t) = E_m \sin(\omega t)\sin^2(\pi t/T). \tag{5}$$

The relationship between the electric field and vector potential is given by

$$E(t) = -(\partial A/\partial t). \tag{6}$$

The Schrödinger equation

$$i(\partial/\partial t)|\psi\rangle = H|\psi\rangle \tag{7}$$

in p-FGH formalism can be written as

$$i\frac{\partial}{\partial t}\psi(k_\mu) = \frac{k_\mu^2}{2m}\psi(k_\mu) + \frac{1}{N}\sum_{j,\nu=1}^{N} V(x_j)e^{-i(k_\mu - k_\nu)x_j}\psi(k_\nu) - \frac{d_1 A(t)k_\mu}{m}\psi(k_\mu), \quad \mu = 1, 2, \ldots, N. \tag{8}$$

In this calculation, only 128 ($=N$) grid points were used [12]. The range of x_j is from 0 to 8 a.u. and of momentum k_μ is -50.3 to $+50.3$ spaced evenly. Diagonalization of the unperturbed Schödinger equation gives 24 bound states and 104 discretized pseudocontinuum states. The first 21 calculated bound-state level energies agree with the exact energy levels up to the eighth decimal places. The 24th bound-state energy is accurate up to the fourth decimal place. To ensure the reliability of the time-dependent p-FGH calculation, we also make a test on an analytically known case [13]. Consider the time-dependent Hamiltonian of a driven harmonic oscillator:

$$H = (p^2/2) + \tfrac{1}{2}\Omega^2 x^2 - qA \cdot p, \tag{9}$$

where the electric field $E(t) = E_m \sin(\omega t)$ and its relationship with $A(t)$ are described in Eq. (6). The transition probability from ground state to excited state $|n\rangle$ is given by the Poisson distribution

$$P_{0\to n} = e^{-\sigma}\sigma^n/n!, \tag{10}$$

where

$$\sigma = \frac{q^2}{2m\Omega}\left|\int_{-\infty}^{\infty} E(t)e^{i\Omega t}dt\right|^2. \tag{11}$$

We integrate the Schrödinger equation by p-FGH with the Bulirsch-Stoer algorithm [14]. Our p-FGH method completely reproduces the exact distribution Eq. (10) up to the given controlled tolerance. So the calibrations of the method on the unperturbed Morse oscillator and the nonperturbative driven harmonic oscillator are both established.

We then propagate Eq. (8) directly in momentum space at frequencies $\omega_1 = 0.0425$ (1074 nm), $\omega_2 = 0.085\,78$ (532 nm), and $\omega_3 = 0.236\,076$ (193 nm), respectively. The pulse duration time T in Eq. (5) is 100 optical cycles. A time step of 0.8 a.u. is used. To prevent wrap-around error from the grid boundaries, a filter function $f(k_\mu) = [1 + \exp(-a|k_\mu - b|)]^{-1}$ with $a = 1.5, b = 40$ is multiplied to the wave function at each time step. The calculated results are convergent with respect to the doubling of the maximum momentum and the number of grid points.

The dissociation probability is defined at the turnoff of the field as

$$P_d = 1 - \sum_{n=1}^{n=24} |\langle\phi_n|\psi(t)\rangle|^2. \tag{12}$$

Because the dissociated fragments are neutral and the pondermotive energy is absent in this process, the minimum momentum value required for dissociation is

$$p = \sqrt{2m(D - |E_{14}|)} \simeq 12.2. \tag{13}$$

The filtered out portions are those components with momenta beyond 40 a.u. and they have a negligible effect on the bound-state projections. Thus, in spite of the filter function, the defined P_d describes the dissociation probability well. In Fig. 2 we plot P_d vs α_0 for all cases, where $\alpha_0 = E_m/m\omega^2$ is the unique parameter of the zeroth-order field-deformed potential that plays the central role at high-frequency limit [1]. For ω_1, at $\alpha_0 = 0.1$ (3.5×10^{15} W/cm^2), $P_d \simeq 3\%$, and at $\alpha_0 = 1.0$ (3.5×10^{17} W/cm^2), $P_d \simeq 96\%$; for ω_2, $P_d \simeq 1\%$, at $\alpha_0 = 0.1$, and $P_d \simeq 87\%$ at $\alpha_0 = 1.0$; while for ω_3, with α_0 up to 1.0 (3.3×10^{20} W/cm^2), P_d is still less than 0.005%. This shows the extreme stabilization of the molecule against dissociation in the high-frequency limit under intense fields. It confirms that the system is stationary at high frequency [1,2].

Next we consider the harmonic-generation effects. It has been shown in real hydrogen atom under an intense field [15] that the acceleration form dipole function gives a better power spectrum than the length form. We use the acceleration form to obtain harmonic-generation spectra in the present case. The expectation value of $\ddot{x}(t)$

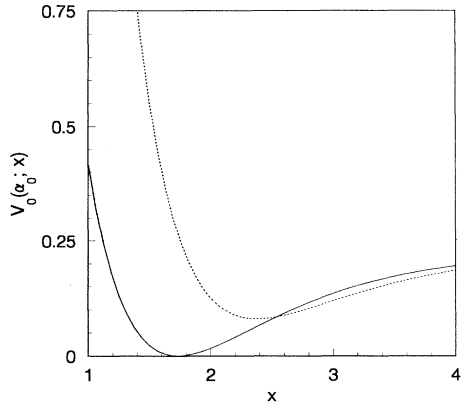

FIG. 1. Field-deformed potential $V_0(\alpha_0; x)$ at $E_m = 3.15$ [corresponds to $\alpha_0 = 1.0$ for ω_1 (1074 nm)]. Dotted line, ω_1 (1074 nm); solid line, ω_3 (193 nm). There is almost no difference from the field-free potential for the latter.

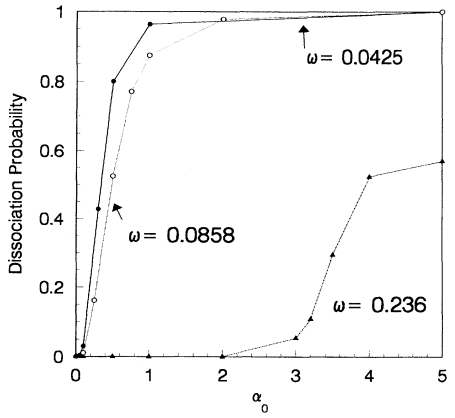

FIG. 2. Dissociation probability vs $\alpha_0 = E_m/m\omega^2$ at ω_1 (1074 nm), ω_2 (532 nm), and ω_3 (193 nm).

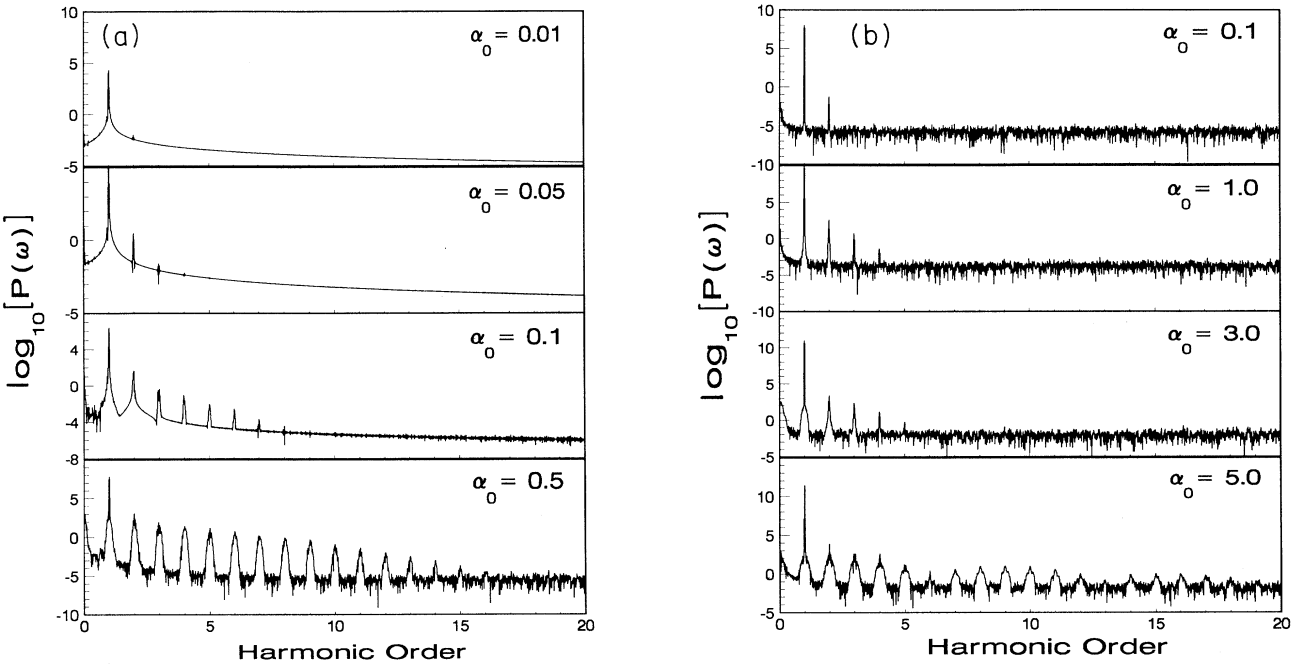

FIG. 3. Harmonic spectrum vs α_0 for (a) 1074 nm and (b) 193 nm.

is obtained by means of Ehrenfest's theorem,

$$m\langle\ddot{x}\rangle = \left\langle -\frac{\partial H}{\partial x}\right\rangle = -2\alpha D\langle e^{-\alpha(x-x_0)} - e^{-2\alpha(x-x_0)}\rangle - d_1 E(t), \tag{14}$$

where in the p representation

$$\langle e^{-\alpha(x-x_0)}\rangle = \frac{1}{N}\sum_{\mu,\nu}\sum_{j}\psi^*(k_\mu;t)e^{-i(k_\mu-k_\nu)x_j} \times e^{-\alpha(x_j-x_0)}\psi(k_\nu;t). \tag{15}$$

The Fourier transform of $\langle\ddot{x}(t)\rangle$ gives a power spectrum of harmonics. We depict in Fig. 3(a) the harmonic spectra for the case ω_1. It shows that at lower field ($\alpha_0 = 0.01$), the motion of the system is just orbiting with laser frequency. High-order harmonics emerge at the increase of laser intensity. At the onset of dissociation ($\alpha_0 = 0.1, P_d \simeq 3\%$), there are harmonics up to order 8. And at high dissociation regime ($\alpha_0 = 0.5, P_d \simeq 80\%$), similar characteristics of atomic harmonic generation appear: an exponential decay in power for the first few orders followed by a plateau region showing nonperturbative behavior [4]. It is interesting to note that the *typical harmonic structure* and *significant dissociation* occur simultaneously. At present, the correlation between these two intense field effects is still an open question [16]. Similar features for the case ω_3 are shown in Fig. 3(b), but the corresponding laser intensities are exceptionally high. For a real molecule in the latter environment the ionization and channel couplings will certainly be more important in making the present model realistic.

To provide a vivid visualization of the time development of the quantum system in phase space (x, p), it is instructive to construct the coarse-grained Wigner (CGW) density distribution [17]

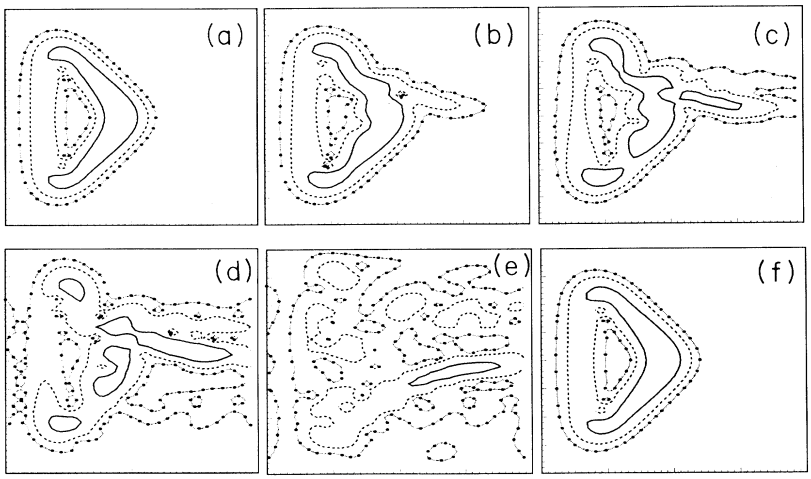

FIG. 4. Contour diagrams at $\alpha_0 = 0.5$, solid line at level 10^{-2}, dashed line at 10^{-3}, and dash-dotted line at 10^{-4}. (a) The initial 14th lowest vibrational state, (b)–(e) time evolution of the initial state under a 1074-nm laser at t=10, 15, 20 and 50 optical cycles, respectively, and (f) for 193 nm at t= 100 optical cycle. The horizontal x axis is from 0 to 8 a.u., while the perpendicular p axis is from −40 to +40 a.u.

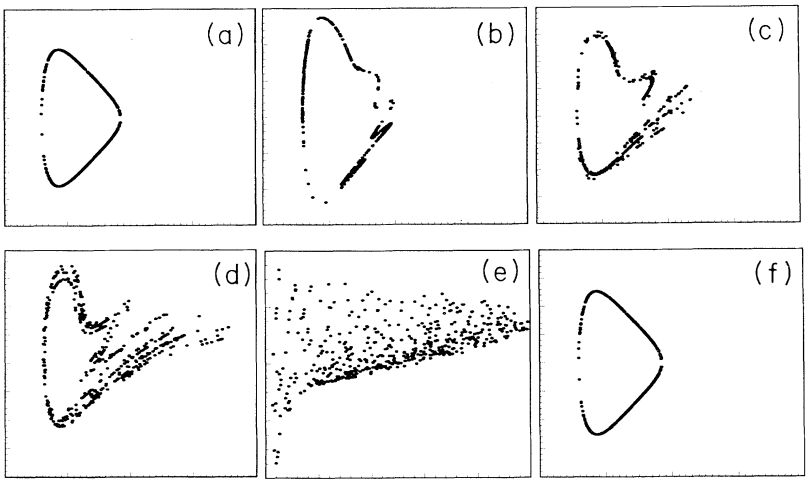

FIG. 5. Classical phase space portraits corresponding to Fig. 4. The x axis and p axis are the same as in Fig. 4, except for (e), where the x axis is 0 to 50 and p axis is -20 to $+60$.

$$\rho(x,p) = (1/2\pi\hbar)|\langle\phi_g|\psi(t)\rangle|^2, \tag{16}$$

where ϕ_g is a coherent state. Figure 4(a) is the contour diagram of the initial 14th lowest vibrational state. Figures 4(b)–4(e) show the time evolution of the initial state under a 1074-nm laser at $\alpha_0 = 0.5$. We can see the breakup of contours and diffusion of the CGW density around the 15th optical cycle. At the 50th optical cycle, the ergodic distribution over the phase space indicates the chaotic behavior. The use of the CGW distribution to describe the chaotic state has been reported before [18]. On the other hand, in Fig. 4(f) we see there is almost no change in the contour structure at $\alpha_0 = 0.5$ during the interaction for 193 nm. The classical correspondences of Figs. 4(a)–4(f) are shown in Figs. 5(a)–5(f). We choose 500 initial points in (x,p) space by Monte Carlo method with the beginning energy equal to the 14th energy level. Then we turn on the field and integrate the classical Hamilton-Jacobi equations. We find that the closed contour starts to break up around the 15th optical cycle, and at the 50th optical cycle the phase-space distribution is chaotic.

In summary, we found that the p-FGH is a very efficient method for solving problems involving the continuum. We examined the stabilization from excited molecular vibrational states in intense fields. Within the currently available frequencies, we showed the stabilization against dissociation at high laser frequency. In the harmonic-generation spectra, we find that the appearance of a plateau in the spectra is related to significant dissociation. The time evolution of the system is shown by both the CGW density distribution and the corresponding classical trajectories. Further details will be reported elsewhere.

The author is thankful for the hospitality of Professor Shih-I Chu through which the study was motivated. He also thanks Y. F. Chen for the frequent discussions and Professor Chii-Dong Lin and Ue-Li Pen for the readings and comments on the manuscript. This work is supported by the National Science Council of Taiwan under Contract No. NSC-82-0208-M009-003.

[1] M. Pont *et al.*, Phys. Rev. Lett. **61**, 939 (1988).
[2] M. Pont and M. Gavrila, Phys. Rev. Lett. **65**, 2362 (1990).
[3] A. Zavriyev *et al.*, Phys. Rev. A **42**, 5500 (1990); B. Yang *et al.*, *ibid.* **44**, R1458 (1991); G.N. Gibson *et al.*, Phys. Rev. Lett. **67**, 1230 (1991); A. Giusti-Suzor and F.H. Mies, *ibid.* **68**, 3869 (1992); M. Saeed *et al.*, *ibid.* **68**, 3519 (1992); R. Heather and H. Metiu, J. Chem. Phys. **88**, 5496 (1988); H.P. Breuer *et al.*, Phys. Rev. A **45**, 550 (1992).
[4] A. McPherson *et al.*, J. Opt. Soc. Am. B **4**, 595 (1987); M. Ferray *et al.*, J. Phys. B **21**, L31 (1988); X. F. Li *et al.*, Phys. Rev. A **39**, 5751 (1989).
[5] See, for example, S. Chelkowski and A.D. Bandrauk, Phys. Rev. A **44**, 788 (1991); A.D. Bandrauk and J. Gauthier, J. Opt. Soc. Am. B **7**, 1420 (1990).
[6] Ue-Li Pen and T.F. Jiang, Phys. Rev. A **46**, 4297 (1992).
[7] C.C. Marston and G.G. Balint-Kurti, J. Chem. Phys. **91**, 3571 (1989); G.G. Balint-Kurti, C.L. Ward, and C.C. Marston, Comput. Phys. Commun. **67**, 285 (1991).
[8] G. Yao and S.I. Chu, Phys. Rev. A **45**, 6735 (1992).
[9] For a discussion on the one-bound-state system and other systems, see M. Gajda, J. Grochmalicki, and M. Lewenstein, Phys. Rev. A **46**, 1638 (1992).
[10] M.E. Goggin and P. Milonni, Phys. Rev. A **37**, 796 (1988).
[11] H.A. Kramers, *Collected Scientific Papers* (North-Holland, Amsterdam, 1956), p. 866; W.C. Henneberger, Phys. Rev. Lett. **21**, 838 (1968).
[12] For comparison with the coordinate space study with the same HF molecule, Chelkowski and Bandrauk in Ref. [5] use 16 384 grid points and Breuer, Dietz, and Holthaus in Ref. [3] use 12 288 points.
[13] C. Cohen-Tannoudji *et al.*, Phys. Rev. A **8**, 2747 (1973).
[14] W.H. Press *et al.*, *Numerical Recipes in Fortran*, 2nd ed. (Cambridge University Press, New York, 1992), p.718.
[15] K. Burnett *et al.*, Phys. Rev. A **45**, 3347 (1992); T.F. Jiang and S.I. Chu, *ibid.* **46**, 7322 (1992).
[16] W. Becker *et al.*, Phys. Rev. A **46**, R5334 (1992).
[17] S.J. Chang and K.J. Shi, Phys. Rev. Lett. **55**, 269 (1985).
[18] See, for example, K. Takahashi and N. Saitô, Phys. Rev. Lett. **55**, 645 (1985); K. Takahashi, J. Phys. Soc. Jpn. **57**, 442 (1988).